BRAIN RESEARCH 1150 (2007) 225–238

available at www.sciencedirect.com

ScienceDirect

www.elsevier.com/locate/brainres

BRAIN RESEARCH

Research Report

Status epilepticus induces region-specific changes in dendritic spines, dendritic length and TrkB protein content of rat brain cortex

Estíbaliz Ampuero[a], *Alexies Dagnino-Subiabre*[c], *Rodrigo Sandoval*[a], *Rodrigo Zepeda-Carreño*[b], *Soledad Sandoval*[a], *Alejandra Viedma*[a], *Francisco Aboitiz*[b], *Fernando Orrego*[a], *Ursula Wyneken*[a,*]

[a]*Neuroscience Laboratory, Faculty of Medicine, Universidad de los Andes, Santiago, Chile*
[b]*Department of Psychiatry and Center for Medical Research, Faculty of Medicine, Pontificia Universidad Católica de Chile, Santiago, Chile*
[c]*Laboratory of Behavioural Neuroscience and Neurobiology, Faculty of Medicine, Universidad Católica del Norte, Coquimbo, Chile*

ARTICLE INFO

Article history:
Accepted 28 February 2007
Available online 7 March 2007

Keywords:
TrkB
Seizure
Neocortex
Dendritic morphology
Apoptosis

ABSTRACT

Induction of status epilepticus (SE) with kainic acid results in a large reorganization of neuronal brain circuits, a phenomenon that has been studied primarily in the hippocampus. The neurotrophin BDNF, by acting through its receptor TrkB, has been implicated in such reorganization. In the present work we investigated, by Western blot and immunohistochemistry, whether regional changes of TrkB expression within the rat brain cortex are correlated with altered neuronal morphology and/or with apoptotic cell death. We found that the full-length TrkB protein decreased within the cortex when measured 24 h to 1 week after induction of SE. Analysis by immunohistochemistry revealed that TrkB staining diminished within layer V of the retrosplenial granular b (RSGb) and motor cortices, but not within the auditory cortex. In layer II/III, differential changes were also observed: TrkB decreased in the motor cortex, did not change within the RSGb but increased within the auditory cortex. Reduced TrkB was associated with dendritic atrophy and decreased spine density in pyramidal neurons within layer V of the RSGb. No correlation was observed between regional and cellular changes of TrkB protein and apoptosis, measured by the TdT-mediated dUTP nick end labeling (TUNEL) method. The global decrease of TrkB within the neocortex and the associated dendritic atrophy may counteract seizure propagation in the epileptic brain but may also underlie cognitive impairment after seizures.

* *Corresponding author*. Ursula Wyneken, Facultad de Medicina, Universidad de los Andes, San Carlos de Apoquindo 2200, Las Condes, Santiago, Chile. Fax: +56 2 2141258.
E-mail address: uwyneken@uandes.cl (U. Wyneken).

Abbreviations: ABC, avidin–biotin complex; BDNF, brain-derived neurotrophic factor; PBS, phosphate-buffered saline; RSGb, retrosplenial granular b cortex; SE, status epilepticus; TUNEL, TdT-mediated dUTP nick end labeling

0006-8993/$ – see front matter © 2007 Elsevier B.V. All rights reserved.
doi:10.1016/j.brainres.2007.02.089

1. Introduction

Epilepsy comprises a collection of disorders whose common feature is a persistent increase in neuronal excitability. In rats, intraperitoneal injection of kainic acid (KA) induces prolonged epileptic seizures (status epilepticus, SE). KA-induced SE is an initial insult that, after a latency period, leads to epilepsy, i.e., the occurrence of spontaneous seizures that is considered an animal model for human temporal lobe epilepsy (TLE). The reorganization of brain circuits following SE is regarded as a key mechanism in epileptogenesis (McNamara, 1999; Pitkanen and Sutula, 2002), i.e., in the development of spontaneous seizures. The hippocampus plays a pivotal role in the initiation and propagation of TLE seizures; therefore, seizure-induced functional and structural alterations have extensively been analyzed in this limbic structure. These include axonal sprouting (Barnes et al., 2003; Scharfman et al., 2003; Bausch and McNamara, 2004; Siddiqui and Joseph, 2005), neuronal loss and neurogenesis (Pitkanen and Sutula, 2002) and changes in dendritic spine morphology (Ribak et al., 2000; Dashtipour et al., 2002; Wong, 2005). In the hippocampus, and especially in the dentate gyrus, it is believed that such reorganization promotes increased excitability and progression of epilepsy. For example, an increase of dendritic spines, that receive the majority of the excitatory synaptic inputs in the brain, as well as axonal sprouting, would contribute to the recurrent excitatory circuitry (Bundman et al., 1994; Ribak et al., 2000; Leite et al., 2005).

Several studies suggest that the neurotrophin brain-derived neurotrophic factor (BDNF), by acting through its cognate receptor TrkB, can contribute to the lasting structural and functional changes underlying limbic epileptogenesis in the adult brain (Binder et al., 2001; Scharfman, 2005). TrkB is a transmembrane tyrosine kinase that becomes phosphorylated when activated. In addition to full-length TrkB, two truncated isoforms, T1 and T2, are expressed: T2 expression is mainly restricted to certain developmental stages, while T1 is expressed mainly in non-neuronal cells in the adult CNS (Goutan et al., 1998; Rose et al., 2003; Silhol et al., 2005). Both isoforms lack their intracellular catalytic domains and are considered dominant-negative isoforms. However, it has recently been shown that they are capable to signal independently from full-length TrkB (Rose et al., 2003). Although TrkB can also be activated by the neurotrophin NT4/5, multiple reports support a role for BDNF, but not for NT4/5, in epileptogenesis. BDNF increases neuronal excitability (Huang and Reichardt, 2003; Rose et al., 2004) and supports the maintenance of cortical neuronal size and dendritic structure, therefore stabilizing neuronal connectivity (McAllister et al., 1995; Gorski et al., 2003; Wirth et al., 2003; Dijkhuizen and Ghosh, 2005; Chakravarthy et al., 2006). These BDNF-mediated actions may have pro-convulsant consequences. At the same time, the survival-promoting signals of TrkB might counteract SE-induced cell death (Huang and Reichardt, 2003; Kalb, 2005).

BDNF and TrkB mRNA and protein are upregulated in the hippocampus following systemic administration of KA, but the pattern and the time course is not uniform among hippocampal subfields: the largest increase of both mRNA and protein occurs in the dentate gyrus, and is long lasting, while the increase in the other hippocampal regions is lower in magnitude and transient (Dugich-Djordjevic et al., 1992; Dugich-Djordjevic et al., 1995; Goutan et al., 1998; Rudge et al., 1998; Katoh-Semba et al., 1999). In addition, TrkB in the mossy fiber pathway appears to be phosphorylated (i.e., activated) during epileptogenesis (Binder et al., 1999; He et al., 2002; Danzer et al., 2004). Data from transgenic mice in which epilepsy is induced by different mechanisms show that conditioned deletion of BDNF did not prevent epileptogenesis in the kindling model. In KA-injected transgenic mice, a larger dose of KA was required to produce limbic seizures. However, when pilocarpine was used for seizure induction, lower doses were effective (He et al., 2004; Barton and Shannon, 2005). Conversely, hippocampal TrkB overexpression exacerbated SE, but not epileptogenesis (Lahteinen et al., 2003). Such studies strongly suggest that increased and activated TrkB has a role in the development and maintenance of hyperexcitable circuits in the hippocampus, although the mechanisms may be more complex than initially thought. It is also less clear whether BDNF/TrkB upregulation extends to neocortical circuits that are localized at distant sites from the epileptogenic focus, and whether TrkB protects against SE-induced cell damage.

The present study was designed to examine the relationship between SE-induced changes in cortical TrkB levels, and the association of such changes with neuronal morphology and fragmented DNA, a marker for apoptotic cell death.

We found that a region-specific TrkB decrease correlated with dendritic retraction. TrkB levels were also diminished within the hippocampal CA1 subfield, where DNA fragmentation is very prominent (Weiss et al., 1996; Tooyama et al., 2002). However, TrkB was upregulated within the piriform cortex, another area particularly sensitive to neuronal damage following KA-induced SE (Sperk, 1994; Tooyama et al., 2002; Freichel et al., 2006), suggesting that TrkB is not related to progression of apoptosis. TrkB downregulation and dendritic retraction may represent compensatory responses of pyramidal neurons to the increased activity levels during SE that tend to minimize further seizure propagation.

2. Results

2.1. *TrkB immunoreactivity within the rat neocortex following SE*

The presence of TrkB protein in the rat cortex was analyzed both by Western blot and by immunohistochemistry. Fig. 1A shows representative Western blots and the quantification of TrkB change in cortical homogenates following SE using an antibody raised against an N-terminal (i.e., extracellular) domain; therefore, both the truncated as well as the full-length isoforms were detected. The full-length receptor began to decrease starting at 24 h after KA injection, while the truncated isoform showed no change up to 3 days. Truncated TrkB diminished in a delayed manner only 1 week after seizures induction. We next analyzed whether full-length TrkB was activated, i.e., phosphorylated. For this, TrkB was immunoprecipitated from cortical homogenates. TrkB was analyzed by Western blot and the membrane re-probed with

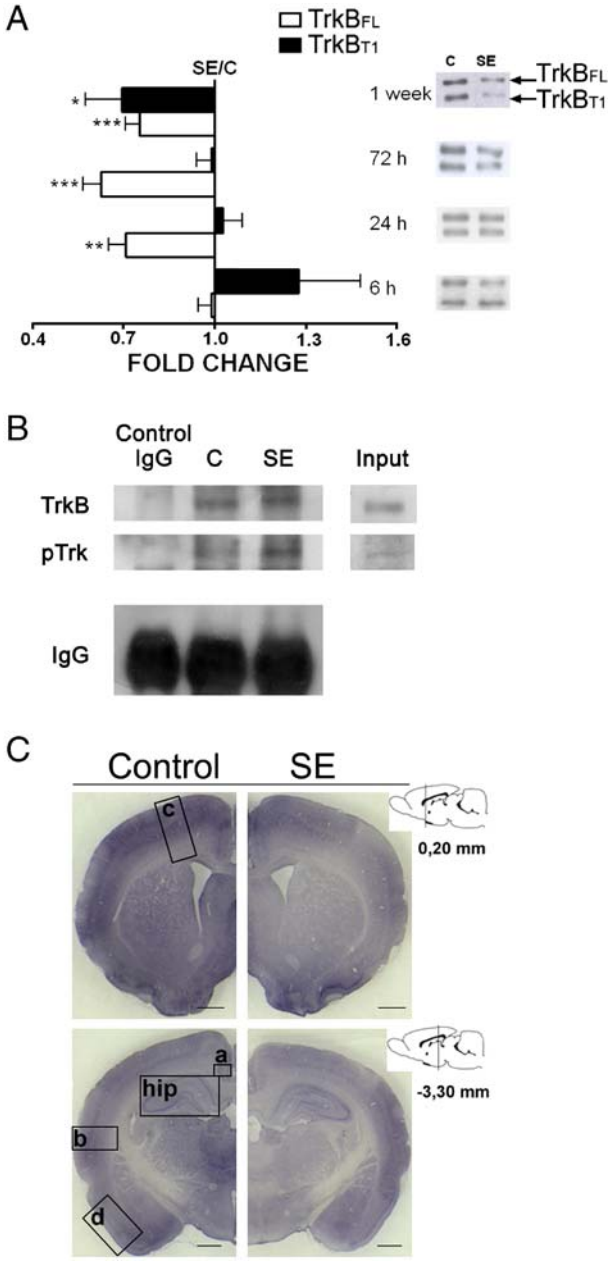

Fig. 1 – $TrkB_{fl}$ decreased within the cortex 72 h after kainic acid-induced status epilepticus (SE). (A) TrkB levels were analyzed in forebrain homogenates by Western blot 6, 24, 72 h and 1 week after seizure induction. $TkB_{full\text{-}length}$ and the truncated isoform were quantified by densitometric analysis. Representative Western blots and fold change from control (C) in five different experimental groups are shown ($^{*}p<0.05$; $^{**}p<0.01$; $^{***}p<0.001$). (B) TrkB immunoprecipitates obtained from cortical homogenates were re-probed for phospho-Trk with an antibody generated against the sequence containing phospho-Y490 of TrkA. (C) Full-length TrkB immunoreactivity was analyzed in coronal forebrain sections. Quantitative analysis was performed within the areas indicated by the following rectangles: (a) retrosplenial granular b cortex (RSGb); (b) auditory cortex; (c) motor cortex; hip: hippocampus; (d) piriform cortex. The insets show the level of the coronal sections. Scale bar: 1 mm.

an anti-phospho-Trk antibody generated against the sequence around Y490 of TrkA (Fig. 1B). The densitometric analysis of the phospho-Trk band indicated that no change in phospho-TrkB could be detected (0.96±0.14; means±SE, $n=3$ independent experiments).

In order to check these results, we performed immunohistochemistry. As the most abundant truncated isoform expressed in the adult central nervous system is T1, that is mostly expressed by non-neuronal cells in the rat forebrain (Goutan et al., 1998; Silhol et al., 2005), we concentrated on the full-length receptor that was recognized by an antibody raised against its intracellular domain. The specificity of the antibody used by us was checked by preincubating the primary antibody (Santa Cruz Biotechnology) with different concentrations of blocking peptide provided by the same company (data not shown). We also used the anti-phospho-Trk antibody ($n=3$).

TrkB protein showed a widespread expression in the forebrain, as already known (Yan et al., 1997). In most cortical areas from control rats, the TrkB protein was predominantly located within layer V cells, but also within layer II/III cells. Layer V cells could easily be identified as pyramidal neurons by their pyriform cell body, the prominent apical dendrite and dendrites arising from the cell body, whereas layer II/III cells appeared to be predominantly granular. Less heavily stained granular neurons could be seen throughout the cortex. In some neocortical regions, e.g., the retrosplenial granular b cortex (RSGb, or area 29C), the apical dendrite of the pyramidal layer V neuron was heavily stained, but in others, like the auditory cortex, dendritic staining was less intense. Immunohistochemistry was performed 72 h after SE because at this time point strong positive TUNEL staining was evident, as seen by us and by others (Lan et al., 2000), allowing a comparison of both phenomena.

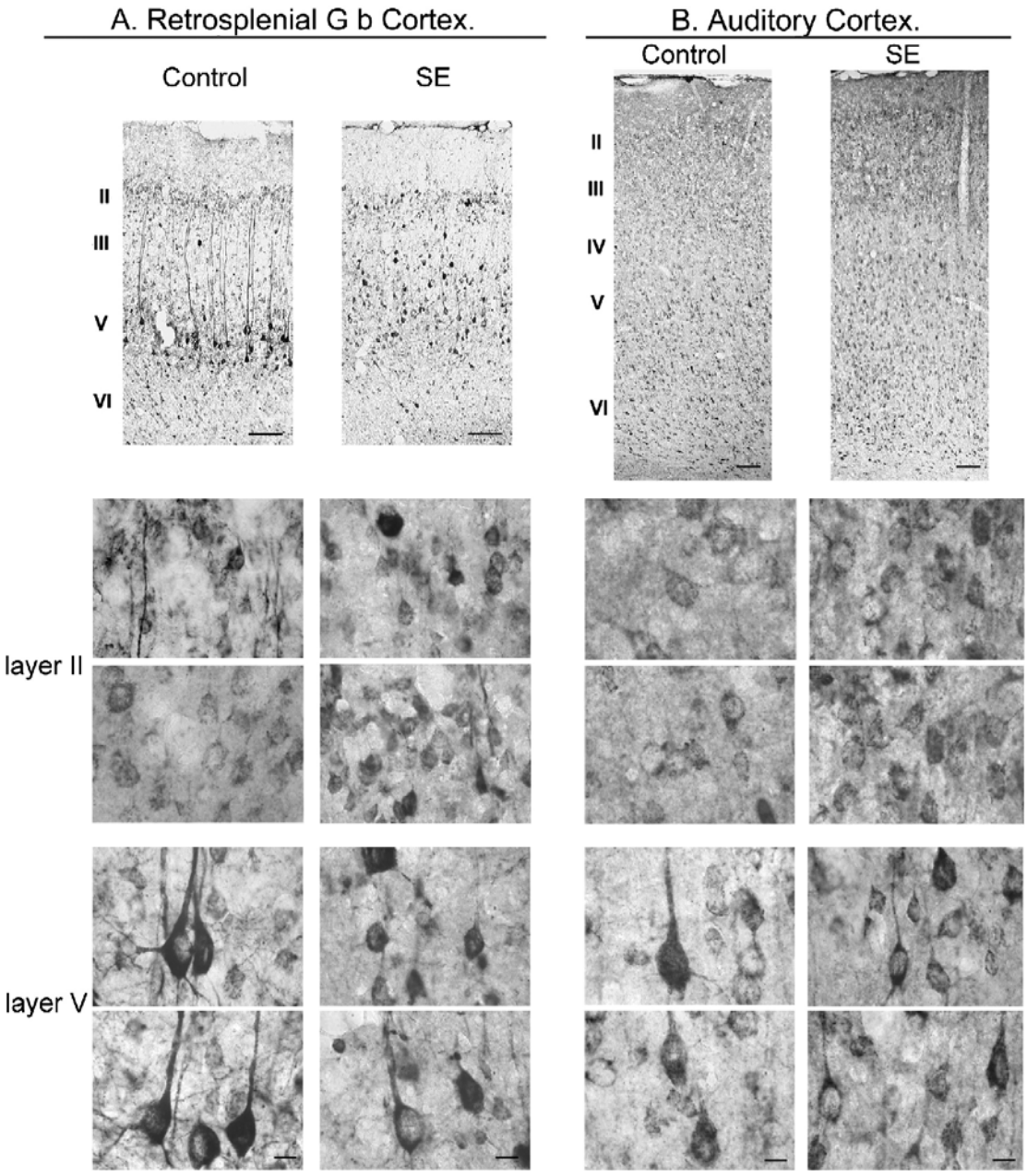

Fig. 2 – TrkB decreased in layer V pyramidal neurons within the RSGb and motor cortices but increased within the piriform cortex 72 h after kainic acid-induced SE. TrkB full-length immunoreactivity was analyzed in coronal forebrain sections. (A) RSGb cortex. (B) Auditory cortex. Different magnifications are shown: Upper panels: low magnification, scale bar = 100 μm. Middle panels: Layer II cells. Lower panels: Layer V cells. Middle and lower panel scale bar: 10 μm. (C) Motor cortex. Scale bars as in panels A and B. (D) Piriform cortex. Scale bar: 100 μm. (E) Upper panel: Total immunoreactivity was quantified in equal areas covering all cortical layers of the RSGb, auditory, motor and piriform cortices of control animals and after SE. The densitometric change after SE over control is shown. Lower panel: a similar analysis was done but restricted to layers V or II/III within the indicated areas.

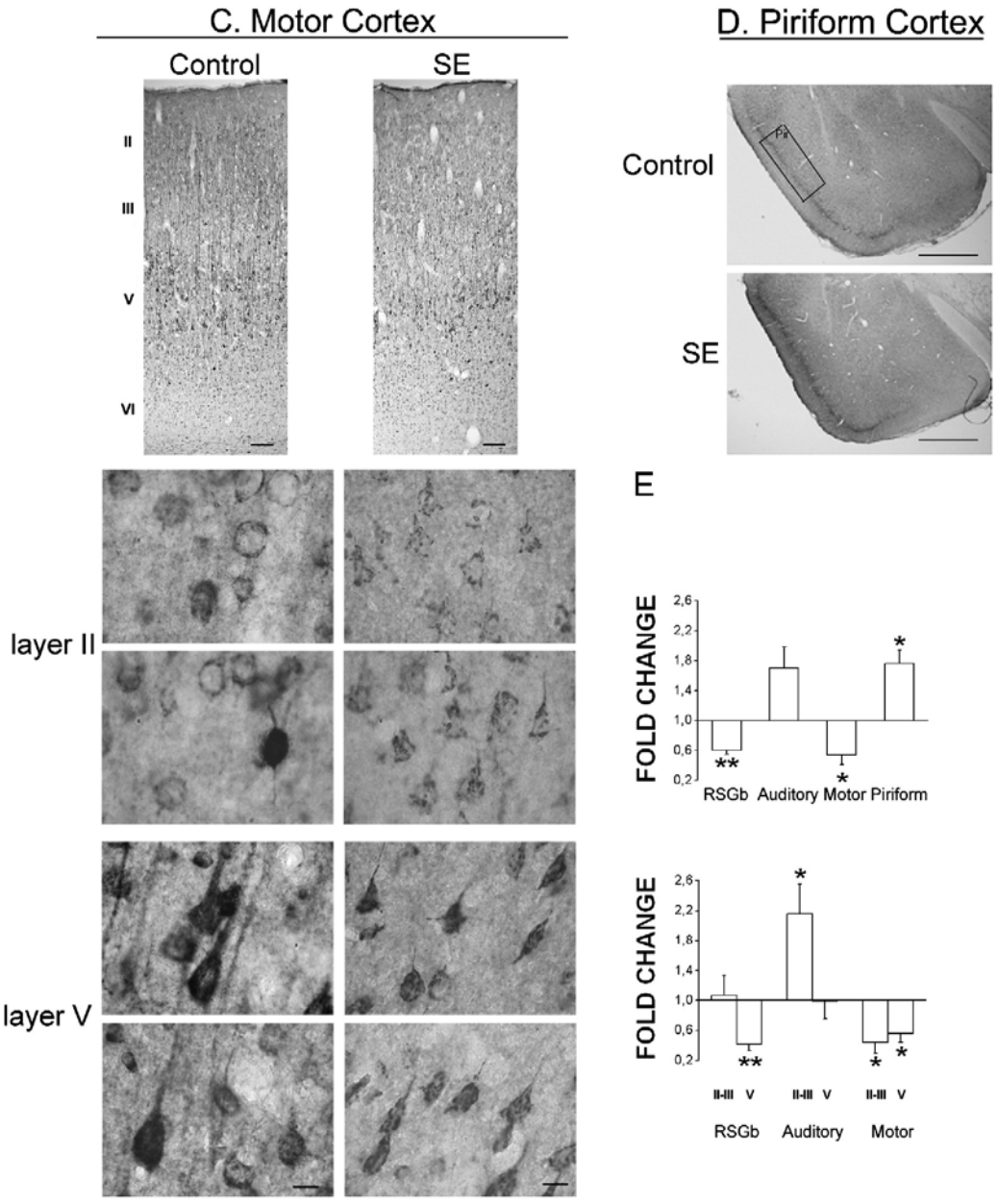

Fig. 2 (*continued*).

After SE, the decrease of total TrkB immunoreactivity could be appreciated in low magnification pictures (Fig. 1C). However, a differential effect of seizures was observed at higher magnification in different cortical regions (Fig. 2). Within the RSGb, a decrease of TrkB immunoreactivity of 39.8±5.2% (mean±SE; $p<0.01$) was observed (Fig. 2E). When analyzing TrkB staining in the more prominently immunopositive cortical layers, a reduction of 58.3±8.7% (mean±SE; $p<0.01$) was observed within layer V, but not within layer II/III (Figs. 2A and E). The decrease was due to less TrkB staining both of the cell soma and the apical dendrites of pyramidal neurons that was accompanied by an evident cell shrinkage (Fig. 2A, lower panel). In contrast, within the auditory cortex, TrkB immunoreactivity did not change within layer V but increased within layer II/III by 115.8±40.1% (mean±SE; $p<0.05$; Figs. 2B and E). Interestingly, layer V pyramidal neurons were less heavily stained following SE, but this seemed to be compensated by a higher proportion of stained cells, as could be appreciated in the high magnification pictures of Fig. 2B. Therefore, the TrkB quantification within this layer showed no net change (Figs. 2B and E, upper panel). The motor cortex revealed a decreased staining within layer II/III by 55.8±14%, and within layer V by 43.8±11.9%. (Figs. 2C and E). Interestingly, granular staining within layer II/III disappeared and pyramidal neurons became immunopositive (Fig. 2C, middle panels). Decrease of TrkB content within layer V pyramidal cells was also associated with pyramidal cell shrinkage (Fig. 2C, lower panel). Finally, within the

piriform cortex, a region that is very susceptible to DNA fragmentation following SE by KA (Weiss et al., 1996; Freichel et al., 2006), TrkB was upregulated by 76.3±17.6% (mean±SE; $p<0.05$; Figs. 2D and E, upper panel).

In the hippocampus, differential changes were also observed: while no change in TrkB immunoreactivity was detected within the dentate gyrus and within the CA3 region, a decrease of 31±12.5% (mean±SE; $p<0.05$) was seen within CA1 (Fig. 5A, lower panel).

We next used anti-phospho-Trk antibody that does not discriminate between phospho-TrkA, TrkB and TrkC. The analysis revealed a very large increase of phospho-Trk in the piriform cortex by 470±131.7% ($n=6$; mean±SE; $p<0.05$), a modest increase in the auditory cortex (141.8±9.1%; $p<0.05$) and no change in the RSGb area. Interestingly, we could not identify cell somas, revealing that most activated Trk was within neuronal processes (not shown). In the hippocampus, as already reported, a large increase of staining was observed

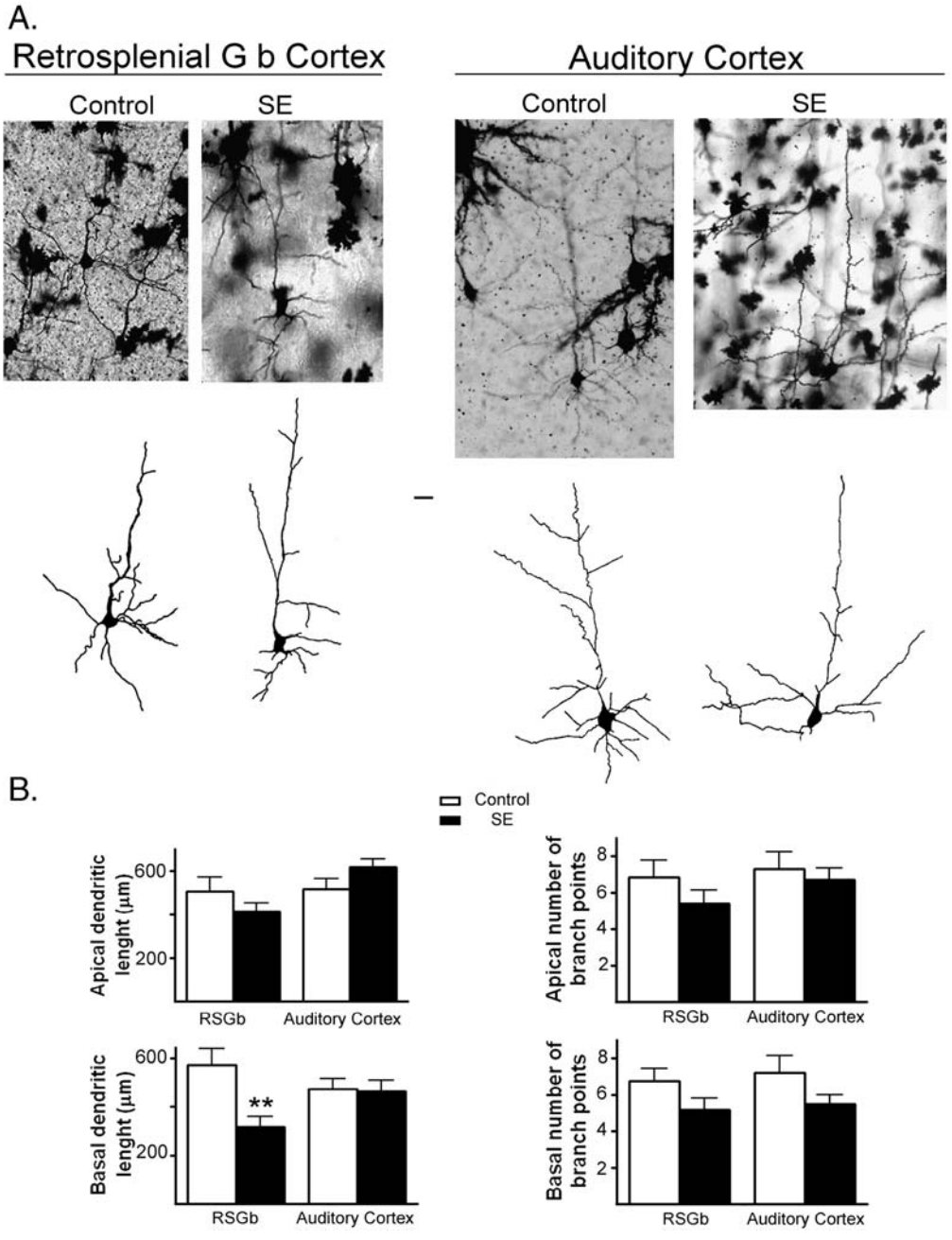

Fig. 3 – Decrease of TrkB within the RSGb correlated with decreased basal dendritic length in Golgi-stain impregnated pyramidal neurons of layer V. (A) Photomicrograph and camera lucida tracings of representative Golgi-stained impregnated pyramidal neurons in the RSGb and auditory cortices of a control rat and a rat after SE. Scale bar: 20 µm. (B) The morphometric analysis shows that the total basal dendritic length was significantly reduced in the RSGb, but not in the auditory cortex ($n=50$ cells; $n=5$ animals), whereas the apical dendritic length did not change.

within the hilus of the dentate gyrus and the CA3 stratum lucidum, and the cell layers were not stained (not shown).

To test whether changes in TrkB were associated with alterations in dendritic morphology and spine density, we analyzed Golgi-impregnated cells from a different set of animals. We compared pyramidal cells within two regions in which opposite overall changes of TrkB immunoreactivity had been observed: the RSGb cortex and the auditory cortex. Fig 3A shows photomicrographs of representative Golgi-impregnated pyramidal neurons from control rats and from rats that had suffered SE. Also, the camera lucida drawings of the selected neurons are shown. We observed an SE-induced reduction of 40.8±3.5% in the length of basal dendrites that was specific to the RSGb cortex (Fig. 3B). No differences were detected in the length of the apical dendrite or number of branch points in both regions. The values of the dendritic length and branch points are the average of at least 12 neurons per region in 5 independent experiments.

The number of spines per 8 μm was measured along a 80-μm segment of the primary apical dendrite, starting from the origin of the branch. Fig. 4A shows representative photomicrographs at 100× and the corresponding camera lucida drawings. The analysis revealed a large decrease of spine density (Fig 4B). In the auditory cortex, the decrease was significant close to the cell soma but returned to control levels at distances greater than 64 μm from the cell body, while within the RSGb area, a significant decrease was observed even at 80 μm from the cell body. Our results show that reduced dendritic length and decreased spine density occurred within layer V pyramidal neurons of the RSGb area, an area where TrkB was downregulated (Fig. 2E).

Finally, we wanted to assess whether regional changes of TrkB levels were associated with DNA fragmentation within forebrain areas that have been reported to be especially susceptible. TUNEL staining was performed in coronal sections at the level of the dorsal hippocampus. In Fig. 5A (upper panel), a hematoxylin counterstain indicating the presence of cell somas in the hippocampal subfields of control animals and of animals following SE is shown. In the lower and right hand panels, the decrease of TrkB in the CA1 subfield is documented. Apoptotic cells were most abundant within the CA1 subfield (58.6±37.1; mean±SE, $p<0.01$), followed by CA3 (15.5±11.5) and the dentate gyrus (3.8±1.1; Fig. 5B). Within the cortex, TUNEL-positive cells were significantly enhanced with respect to controls in the piriform cortex (10.5±1.2 nuclei per area of 5712 m^2; mean±SE, $p<0.001$) and in the auditory cortex (2.3±0.6 nuclei per area of 5712 μm^2; $p<0.05$). Interestingly, two forebrain regions with high

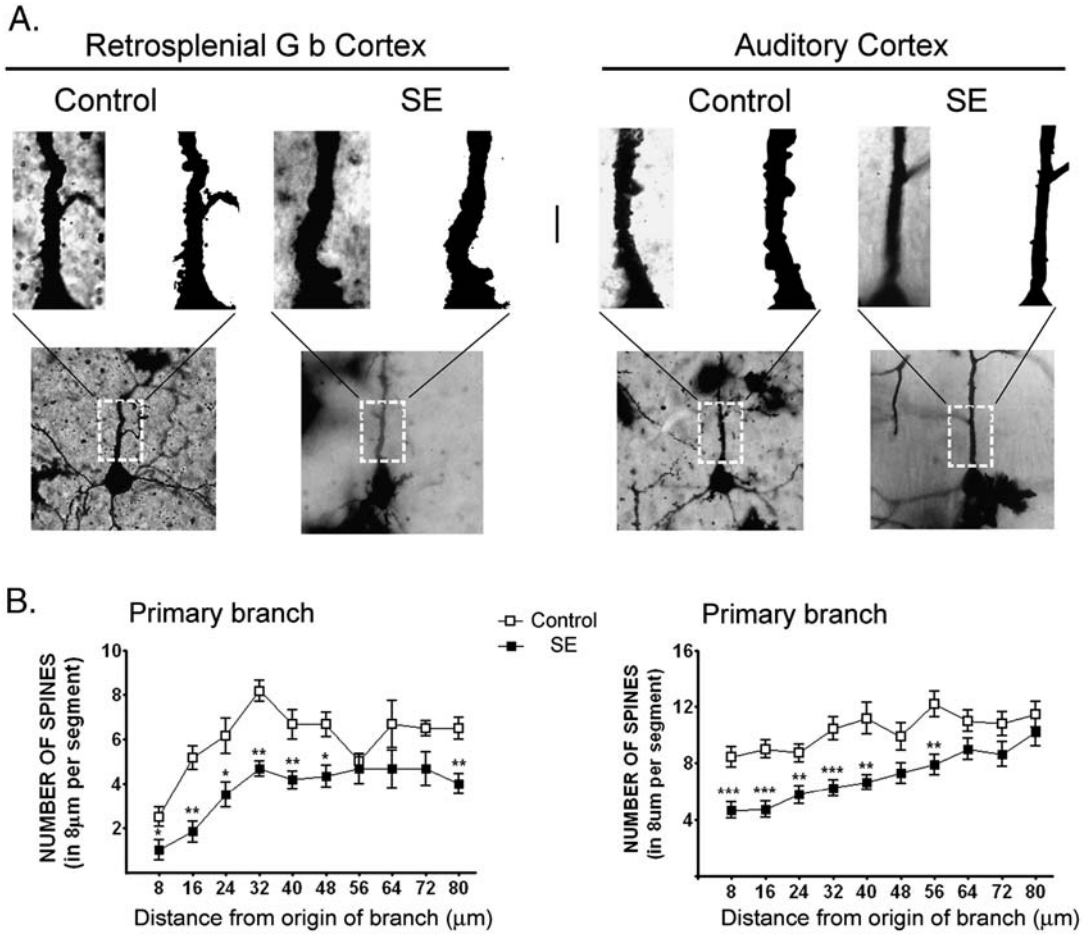

Fig. 4 – Effect of SE on spine density in pyramidal neurons of layer V. (A) Low and high magnification representative photomicrographs of Golgi-stained primary apical dendrites are shown. Scale bar (upper panel): 8 μm (B) Quantification of spine density showed a decrease within both regions after SE. At 80 μm from the origin of the cell body, the decrease continued to be significant within the RSGb, but not within the motor cortex.

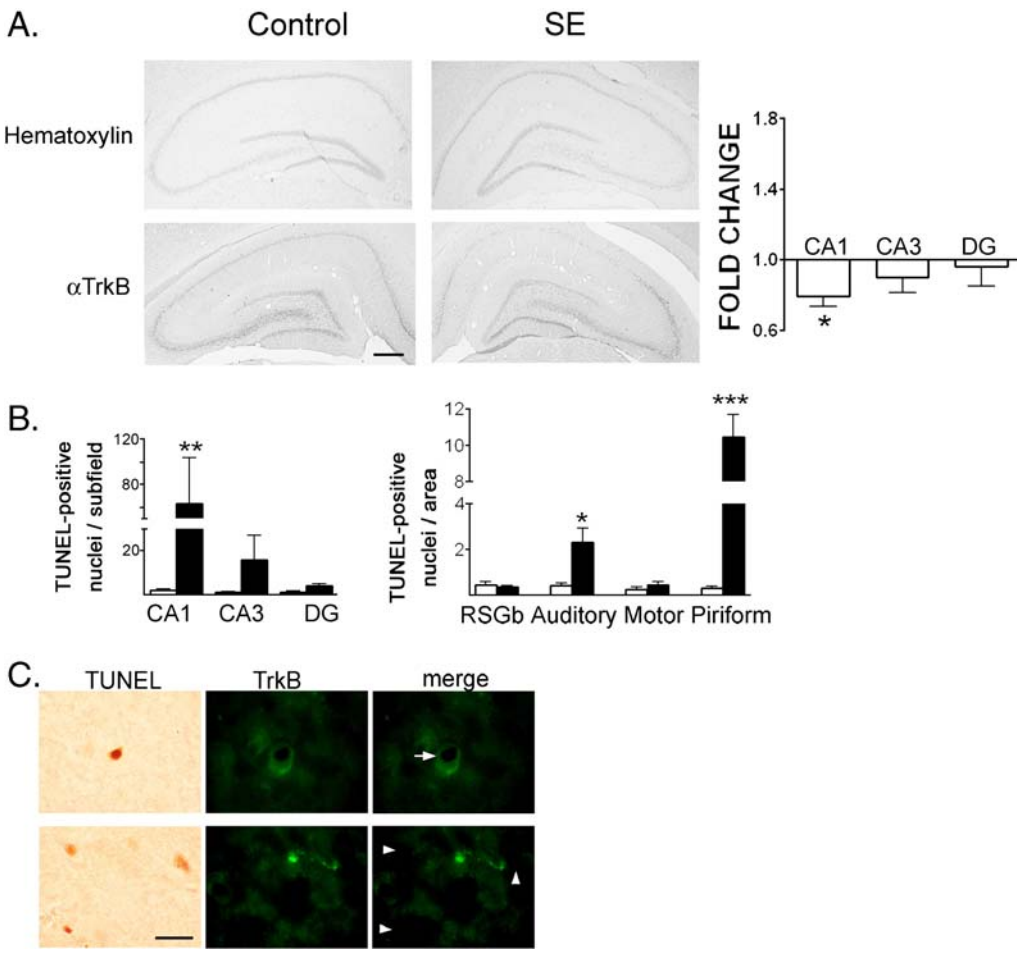

Fig. 5 – Cells bearing fragmented DNA, revealed by the TUNEL method, are increased within the piriform cortex and CA1 hippocampal region 72 h after KA injection. (A) Upper panel: hematoxylin staining is shown to assess that no gross morphological alterations occur in the hippocampus after SE (right panel) when compared with control (left panel). Lower panel: TrkB immunoreactivity in the hippocampus is shown. At the right side, the fold change of TrkB immunoreactivity within each hippocampal subfield is shown, indicating a decrease within the CA1 subfield. (B) Quantification of TUNEL-positive nuclei in control sections and after SE ($n=5$ control and 13 experimental rats). The number of stained nuclei was counted within each hippocampal subfield (left panel) and within rectangles of 5,712 μm^2 within the indicated cortical areas. (C) After performing the TUNEL reaction, TrkB was immunostained using a fluorescent secondary antibody. Some cells were positive for both TrkB and TUNEL, indicated with an arrow, while others were only TUNEL-positive (arrowheads). Scale bar: 40 μm.

TUNEL staining showed either a decrease (CA1 subfield) or an increase (piriform cortex) in TrkB levels. When colocalization of TrkB and TUNEL staining was analyzed at the cellular level in the piriform cortex using a fluorescent secondary antibody to detect TrkB ($n=3$), we found that 27.8±9.1% of TUNEL-positive cells also showed TrkB immunostaining. Fig. 5C shows apoptotic cells that were positive for TrkB (arrow, upper panel) or negative for it (arrowheads, lower panel). These results suggest a lack of protection mediated by BDNF/TrkB signaling on progression of neuronal death by apoptosis both at the regional as at the cellular level.

3. Discussion

Our experiments show that TrkB levels decrease in the rat brain cortex after induction of SE with KA. However, in the piriform cortex, a region implicated in the propagation of seizures and epileptogenesis, both TrkB and phospho-Trk were increased. Thus, our study confirms that exacerbated TrkB signaling might promote epileptogenesis, while its down-regulation might represent a form of homeostatic plasticity that adequates cortical connectivity to enhanced activity. Our results may help to explain why some brain areas are resistant to the development of epilepsy while others are not. Because decreased BDNF/TrkB signaling is also associated with cognitive impairment (Hariri et al., 2003; Bekinschtein et al., 2007; Heldt et al., 2007), it would be highly interesting to find out whether differential downstream mechanisms of TrkB are involved in epileptogenesis and functions like learning and memory. A better understanding of endogenous mechanisms that are able to counteract the development of epilepsy following a brain insult may have important therapeutic applications in the future.

3.1. *Total decrease of TrkB in rat brain homogenates*

The overall decrease of TrkB protein level in the brain cortex contrasts with the reported upregulation of BDNF/TrkB and phospho-TrkB in the hippocampal CA3 area and dentate gyrus, where it is thought to be involved in temporal lobe epileptogenesis (Dugich-Djordjevic et al., 1995; Goutan et al., 1998; Danzer et al., 2004). In agreement with our results, Goutan et al. (1998) also found diminished TrkB levels within the CA1 region. The differential changes of TrkB protein in hippocampal subfields led to no net change in TrkB protein in hippocampal homogenates (Danzer et al., 2004). Therefore, the decrease observed by us in cortical homogenates might reflect decreased TrkB levels in large forebrain regions. Although TrkB diminished, the phospho-TrkB content did not significantly change in immunoprecipitates. This result may be influenced by the very large increase of phospho-Trk within the piriform cortex, that may in part be phospho-TrkB, and by modest increases of phosphor-TrkB in other cortical areas. An immunohistochemical analysis with a specific anti-phospho TrkB antibody, at this time not available commercially, would help to clarify whether the region-specific decrease of TrkB levels is accompanied by diminished phospho-TrkB. The results obtained with our experimental strategy strongly suggest that increases in TrkB levels are accompanied by large increases of its activated form in the piriform cortex. However, a decrease of TrkB was accompanied by no evident change in its phosphorylation level in the RSGb. It would be very difficult to detect a decrease of phospho-Trk in this region because the staining intensity is very near to background levels. In conclusion, the experimental strategy to find out where TrkB is activated needs to be refined.

On the other hand, truncated TrkB levels tended to increase at 6 h and its downregulation was delayed beyond full-length TrkB. It has been proposed that truncated TrkB might restrict the availability of BDNF to neurons, thereby limiting dendritic and neuritic growth (Dugich-Djordjevic et al., 1995). This would constitute another neuroadaptive response to SE in the brain cortex.

The overall decrease of TrkB within the neocortex is in apparent conflict with data previously published by us, in which it was seen that following seizures, TrkB associates importantly with the postsynaptic density, a specialization of the postsynaptic membrane at excitatory synapses (Wyneken et al., 2001; Wyneken et al., 2003). We now isolated postsynaptic densities from the rat forebrain 72 h following seizures and found that the TrkB content in them continued to be increased by 377 ± 60% (not shown). This result and the appearance of punctate TrkB staining, that can be visualized, e.g., within the motor cortex (Fig. 2C), indicates that the subcellular localization of TrkB following SE changes. The insertion of TrkB to postsynaptic densities may have important consequences on synaptic function that we are investigating (manuscript in preparation).

3.2. *Regional changes of TrkB levels 72 h following kainic acid injection*

Following seizures, TrkB decreased in pyramidal cell dendrites and their soma. However, scattered non-pyramidal cells across all cell layers became TrkB positive. Within layer II of the motor cortex, most TrkB immunopositive cells in control animals seemed to be granular, whereas following SE, pyramidal neurons became immunopositive. Taken together, these results show that the overall responsiveness to BDNF decreases in the cortex, excluding the piriform cortex, but also that the cell type that is able to transduce the neurotrophin signal changes. This may have consequences on the stability of specific cortical circuits and thus, information processing, that needs to be further investigated. Decreases within layer V pyramidal cells may affect the "health" of subcortical projections and their targets. For example, pyramidal layer V neurons of the limbic RSGb cortex, that showed a 58.3% decrease of TrkB immunoreactivity, project to the subiculum (Wyss and Van Groen, 1992; Van Groen and Wyss, 2003). As axon morphology is also regulated by BDNF and TrkB (Hanamura et al., 2004; Koyama et al., 2004), the decrease of TrkB in projecting neurons may produce retraction of efferent pathways leading to deafferentation, e.g., of the hippocampus, and to deleterious functional consequences, as impairment of learning and memory, functions in which both structures and their reciprocal connections have been involved (van Groen et al., 2004).

3.3. *TrkB and its relationship with dendritic morphology*

TrkB is known to modulate importantly dendritic branching and dendritic spine morphology (McAllister et al., 1995; Huang and Reichardt, 2003; Chakravarthy et al., 2006; von Bohlen und Halbach et al., 2006). Dendritic branching and spine density determine the efficacy by which synaptic information, especially that mediated by the excitatory neurotransmitter glutamate, is transmitted to the soma (Whitford et al., 2002). Spines in the neocortex are found at a linear density of 1–10 spines per μm of dendritic length in mature neurons. They are considered to be remarkably dynamic structures, changing their size, shape and density in relation to synaptic plasticity (Hering and Sheng, 2001). This might extend to plasticity following SE. We found a significant reduction in basal dendritic branching in the RSGb cortex, while no change was observed within the auditory cortex. In contrast, spine density decreased in both the RSGb and in the auditory cortex. The decrease of TrkB in the layer V RSGb cortex was therefore associated with overall dendritic retraction. In the auditory cortex, where layer V immunoreactivity did not change, a detailed examination suggests that the expression of TrkB in individual pyramidal neurons decreased, and this was associated with soma shrinkage, while the proportion of immunoreactive cells increased. This may help to explain why spine density is also decreased in pyramidal neurons within this area. In a different experimental model, in which focal neocortical seizures were induced, minimal effects on dendritic spines were observed (Rensing et al., 2005). However, we could clearly show that in the KA model of TLE, a large reduction in spine density is observed within the neocortex, far away from the epileptic focus. We propose that decreased TrkB within the cortex may in part mediate spine retraction. The relationship between spine abnormalities and cognitive impairment has extensively been documented (Fiala et al., 2002; Wong, 2005). It is possible that the widespread decrease

in dendritic spines may represent a structural substrate and mechanistic basis for cognitive deficits following seizures (Wong, 2005).

3.4. *Apoptosis following KA-induced SE*

Our observations that cell loss is more prominent within both the CA1 region and the piriform cortex following KA-induced SE had been reported previously (Weiss et al., 1996; Siddiqui and Joseph, 2005), although a high interindividual variability has been detected by us and by others (Sperk, 1994). From the nine rats analyzed by us, three showed abundant TUNEL-positive nuclei in both the piriform cortex and the CA1 subfield. Increased apoptosis within two regions that show opposite changes of TrkB levels strongly suggest that both phenomena occur independently. This is supported by the observation that, at the cellular level, about 30% of cells undergoing apoptosis expressed TrkB while others did not. In that line, studies in mice with forebrain-restricted deletion of BDNF that suggest that TrkB signaling is required for the maintenance of neuronal morphology, but not for cell survival (Gorski et al., 2003). Interestingly, BDNF/TrkB protected a hippocampal cell line from serum deprivation-induced cell death but not from glutamate-induced cell death, suggesting that the survival-promoting activity of BDNF is restricted (Rossler et al., 2004). In addition, the lack of other growth factors that have been shown to support the survival of neurons may be more closely associated with apoptosis following SE than a decrease of BDNF/TrkB signaling (Lindholm et al., 1996; Yoo et al., 2006).

Our study opens new and interesting questions in the field that should be addressed in the future: (1) Which are the consequences of changes in TrkB levels on synaptic structure and function? (2) Which is the chemical identity of neurons that newly express TrkB within the cortex? (3) Why is TrkB regulated in opposite directions in different brain regions that are subjected to the same initial insult? (4) Is the downregulation of TrkB essential to avoid epileptogenesis in resistant cortical areas?

TrkB-induced morpho-functional reorganization in the hippocampal network during epileptogenesis may constitute the substrate for the generation of neuronal discharges that spread over the cortex once temporal lobe epilepsy has developed. Similarly, increased levels of TrkB within the piriform cortex may participate in the amplification and propagation of limbic forebrain seizures (McIntyre and Kelly, 2000; Schwabe et al., 2004). However, other brain regions may develop adaptive responses that tend to restrict the propagation of epileptic activity. Our morphological studies show that the neocortex adapts to the new activity levels by a retraction of those structures that receive excitatory input, that is, dendrites and dendritic spines, and that such changes may in part be due to TrkB downregulation.

4. Experimental procedure

4.1. *Materials*

All chemical reagents were purchased from Sigma (St. Louis, MO, USA), unless otherwise stated. Kainic acid was from Ocean Produce International (Canada). TrkB primary antibody against the intracellular domain of TrkB for immunohistochemistry and the blocking peptide were from Santa Cruz Biotechnology (sc-12 and sc-12P, Santa Cruz, CA, USA), whereas the antibody for Western blot that recognized the extracellular domain of TrkB was from BD Biosciences (San Jose, CA, USA). Anti-TrkB for immunoprecipitation was from Upstate (Lake Placid, NY, USA) and anti-phospho-Trk antibody (against tyrosine 490 of TrkA) was from Cell Signaling (ON, Canada). Horseradish peroxidase-conjugated secondary antibodies were provided by BioRad (Hercules, CA, USA) and biotinylated anti-rabbit IgG was from Jackson ImmunoResearch Laboratories (West Grove, PA, USA). Fluorescent goat anti-rabbit IgG linked with Alexa fluor 488 was from Invitrogen (Carlsbad, CA, USA). In Situ Apoptosis Detection Kit NeuroTACS™ was from R and D Systems (Minneapolis, USA). The avidin–biotin horseradish peroxidase complex was from Vector Laboratories (ABC Vectastain Elite Kit; Burlingame, CA, USA). The FD Rapid GolgiStain™ kit was from FD Neuro Technologies, Inc. (Ellicott City, MD, USA).

4.2. *Animals*

Adult male Sprague–Dawley rats (250–300 g) were used in all the experiments. Procedures involving animals and their care were performed in accordance with the National Research Commission guidelines and the Universidad de los Andes Ethical Committee. All efforts were made to minimize animal suffering.

4.3. *KA-induced status epilepticus*

KA (10 mg/kg dissolved in saline) or saline alone was administered intraperitoneally. The rat's behavior was observed continuously for 6 h thereafter, and seizures were classified as done previously (Wyneken et al., 2001). Only animals suffering generalized seizures (stages 5 and 6, bilateral forelimb clonus with rearing and loss of postural control) for at least 30 min were used for subsequent experiments.

4.4. *Western blots*

Rats ($n=5$ control and $n=5$ KA injected for each time point) were killed at different times after KA injection (6, 24, 72 h and 1 week). Brains were quickly removed, and the cortex of each animal was homogenized separately in 5 ml/g wet weight of homogenization buffer [0.32 M sucrose, 5 mM HEPES, 0.5 mM EGTA, pH 7.4, containing a protease inhibitor mixture (Boehringer Mannheim)]. Twenty micrograms of protein was dissolved at 1 mg/ml in gel loading buffer, separated by sodium dodecylsulfate polyacrylamide electrophoresis (SDS–PAGE) on 5–20% gels under fully reducing conditions and transferred onto nitrocellulose membranes. Membranes were incubated overnight with primary antibody followed by incubation with horseradish peroxidase-conjugated secondary antibody. Immunoreactivity was visualized using the ECL detection system (Amersham Biosciences). Quantification was performed by densitometric analysis of the specific bands and expressed as fold change over control.

4.5. *Immunoprecipitation*

Two hundred micrograms of homogenate was solubilized during 2 h in solubilization buffer (50 mM Tris–HCl pH 9.0, 1% deoxycholate plus proteases inhibitors), under constant agitation at 4 °C. The remaining particulate material was discarded by centrifugation (5 min at 9500×*g*) and 6 μg of anti-TrkB antibody or control IgG was added to each supernatant to interact overnight at 4 °C. Subsequently, 20 μl Protein G Sepharose (pre-washed with solubilization buffer and blocked with 0.2% BSA) was added and incubated for 1 h at 4 °C under agitation. The samples were centrifuged for 5 min at 1000×*g* and the supernatants were discarded. The immunoprecipitates were washed three times with solubilization buffer and were resuspended in 60 μl of electrophoresis loading buffer.

4.6. *Immunohistochemical analysis of TrkB and pTrk*

A different set of rats, including control ($n=6$) and KA-injected ($n=7$) groups, were used for the immunohistochemical analysis of TrkB. Seventy-two hours after KA injection, each rat was sacrificed under ketamine (50 mg/kg) and xylazine (5 mg/kg) anesthesia, perfused intracardially with 0.9% saline followed by 300 ml of 4% buffered paraformaldehyde solution. Afterwards, the rats were decapitated and the brain was removed immediately and subsequently cryopreserved sequentially in 10% and 30% sucrose. The brain was cut serially in 30-μm frozen coronal sections. Free floating sections were washed once in 0.1 M PBS for 10 min, followed by two times of incubation in 0.5% H_2O_2 for 15 min. Then, sections were washed in 0.1 M PBS two times for 10 min, and nonspecific binding blocked in blocking solution (5% normal goat serum (NGS), 0.02% sodium azide, 0.1% bovine serum albumin (BSA), 0.4% Triton X-100 in 0.01 M PBS, pH 7.4) for 1 h, followed by incubation for 72 h at 4 °C with agitation in the presence of the primary antibody (1:4000 for anti-TrkB and 1:1000 for anti-pTrk). After this, the sections were washed six times in 0.01 M PBS for 10 min and incubated with secondary antibody (1:1000) for 2 h in blocking solution. Sections were washed four times in 0.01 M PBS for 10 min and then incubated for 1.5 h at room temperature with ABC in PBS (1:500). For the development of color reaction, the sections were incubated for 8 min at room temperature, with 0.05% 3,3′-diaminobenzidine (DAB), 0.01% H_2O_2, 0.15 % $NiCl_2$ in Tris–saline buffer (50 mM Tris–HCl, 150 mM NaCl, pH 7.6), yielding a dark purple staining. The specificity of the primary antibody was tested either by omitting the primary antibody or by preincubating the primary antibody with the TrkB-blocking peptide provided by Santa Cruz. This resulted in disappearance of staining in a concentration-dependent manner (not shown). For colocalization of TrkB with TUNEL-positive cells, we used the goat anti-rabbit IgG linked with Alexa fluor 488 at 1:200 dilution. Finally, sections were mounted on glass slides with gelatin (0.1%), dried overnight and coverslipped with Entellan (Merck, Germany). Photography used ordinary light or fluorescence on a Zeiss axiophot epifluorescent microscope. Some sections were counterstained with hematoxylin (Sigma) for observation of cell morphology.

TrkB and pTrk-like immunoreactivity was quantified in the hippocampus and neocortex in coronal sections, restricted to those located between interaural 9.20 mm and bregma 0.20 mm for rostral sections and interaural 5.7 mm and bregma −3.30 mm for medial sections (Paxinos and Watson, 1997). Brain slices were visualized under a light microscope (Axioscope, Zeiss, Germany), and images (×2.5, ×10 and ×100 magnifications) were captured with a digital camera (Nikon, Coolpix 995). Digitized images were analyzed with the Unscanit program. Intensity of TrkB-like immunoreactivity was analyzed in equal sample areas of a size that depended on the analyzed region (Fig. 2A). In each hippocampal subfield, the densitometric analysis was done in ten individual samples of 10 μm^2 each, giving a mean intensity value. The background signal originated from DAB-labeled probes was measured in a nonlabeled contiguous area out of the analyzed region and was subtracted from the respective positive values.

4.7. *In situ TUNEL staining*

Seventy-two hours after kainic acid injection ($n=13$ rats) and in control animals ($n=5$), terminal deoxynucleotidyltransferase (TdT)-mediated dUTP–biotin nick end labeling (TUNEL) assay was performed in sections at interaural 5.7 mm and bregma −3.30 mm (Paxinos and Watson, 1997) using the NeuroTACS™ In Situ Apoptosis Detection Kit, according to the manufacturer's instructions. DNA breaks in floating coronal sections were labeled by incubation of 100 μl of TdT and nucleotide mixture containing biotin-conjugated dUTP for 60 min at 37 °C followed by incubation with streptavidin-conjugated horseradish peroxidase. This generates a black precipitate in the presence of DAB and $NiCl_2$ 0.15 M. For co-localization of TUNEL and TrkB, TUNEL immunohistochemistry was followed by fluorescent staining of TrkB. The percentage of TUNEL-positive cells that expressed TrkB was calculated as follows: number of co-stained cells × 100/number of TUNEL-positive cells. Some sections not stained for TrkB were counterstained with hematoxylin to aid in the morphological verification of cells. Within the cortex, apoptotic nuclei, containing dense round apoptotic bodies and condensed dark nuclear ball-like precipitate, were counted under ×100 magnification over 25 (control) or 75 (after SE) fields (5,712 μm^2). Within the hippocampus, the number of apoptotic nuclei was counted per each subfield.

4.8. *Morphological analysis*

A different set of rats, including control ($n=6$) and KA-injected (72 h following injection, $n=7$) groups, was used for morphological analysis.

After perfusion, the brain was removed quickly and processed using FD Rapid GolgiStain™ kit. Briefly, brains were placed in Golgi–Cox solution and stored in the dark for 14 days, after which they were placed in 30% sucrose at 4 °C for 2 days before being sectioned. Coronal sections were cut at 120 μm on a sliding cryostat (Microm, Walldorf, Germany). Sections were collected serially, dehydrated in absolute alcohol, cleared in xylene and coverslipped with Entellan (Merck, Germany). Slides were coded before quantitative analysis, and the code was broken only after the analysis was completed. The morphometric analysis of pyramidal neurons of layer V of both retrosplenial granular b cortex (RSGb) and

the primary auditory cortex (Au1) were restricted to interaural 5.86 and bregma −3.14 and interaural 5.2 mm and bregma −3.8 mm, respectively (Paxinos and Watson, 1997). Pyramidal neurons were defined by the presence of a basilar dendritic tree, a distinct, single apical dendrite and dendritic spines. Neurons with somata in the middle third of sections were chosen to minimize the number of truncated branches. The experimenter selected independently and at random 10 neurons in the RSGb and the auditory cortex for each animal, which fulfilled the following selection criteria: (1) presence of untruncated dendrites, (2) consistent and dark impregnation along the entire dendritic field and (3) relative isolation from neighboring impregnated neurons to avoid overlap. In order to reduce error in data acquisition and self-deception by the experimenter, the latter had no knowledge of whether the sample analyzed was from a control or a KA-injected rat, but they unavoidably knew whether the sample was from the RSGb or the auditory cortex. Camera lucida tracings (500×, BH-2, Olympus Co., Tokyo, Japan) were obtained from selected neurons and then scanned (eight-bit grayscale TIFF images with 1200 dpi resolution; EPSON ES-1000C) along with a calibrated scale for subsequent computerized image analysis. Custom-designed macros embedded in SCION Image (NIH) software were used for morphometric analysis of digitized images. In each selected neuron, the dendritic length and the number of branch points were determined.

Dendrites directly originating from cell soma were classified as primary dendrites. Starting from the origin of the branch, and continuing away from the cell soma, spines were counted along a 80-μm stretch of the dendrite. This 80-μm length was further divided into 10 steps of 8 μm each. The number of spines for each 8-μm segment, at a given distance from the origin, was then averaged across all neurons in each experimental group. All protrusions, irrespective of their morphological characteristics, were counted as spines if they were in direct continuity with the dendritic shaft.

4.9. *Statistical analysis*

Western blots and immunohistochemistry for TrkB were analyzed by a one sample *t*-test with the Graph Pad Prism4 software. The morphological and TUNEL studies were analyzed using a Mann–Whitney *U*-test. Results were presented as the mean ± SEM of six or seven independent experiments. A probability level of 0.05 or less was accepted as significant.

Acknowledgments

We are grateful to Mauricio Sandoval for careful reading of this manuscript. This work was supported by Farmacias Cruz Verde, by Fondecyt 1020257 (to U.W.) and by Universidad de los Andes.

REFERENCES

Barnes, G., Puranam, R.S., Luo, Y., McNamara, J.O., 2003. Temporal specific patterns of semaphorin gene expression in rat brain after kainic acid-induced status epilepticus. Hippocampus 13 (1), 1–20.

Barton, M.E., Shannon, H.E., 2005. The seizure-related phenotype of brain-derived neurotrophic factor knockdown mice. Neuroscience 136 (2), 563–569.

Bausch, S.B., McNamara, J.O., 2004. Contributions of mossy fiber and CA1 pyramidal cell sprouting to dentate granule cell hyperexcitability in kainic acid-treated hippocampal slice cultures. J. Neurophysiol. 92 (6), 3582–3595.

Bekinschtein, P., Cammarota, M., Igaz, L.M., Bevilaqua, L.R., Izquierdo, I., Medina, J.H., 2007. Persistence of long-term memory storage requires a late protein synthesis- and BDNF-dependent phase in the hippocampus. Neuron 53 (2), 261–277.

Binder, D.K., Routbort, M.J., McNamara, J.O., 1999. Immunohistochemical evidence of seizure-induced activation of trk receptors in the mossy fiber pathway of adult rat hippocampus. J. Neurosci. 19 (11), 4616–4626.

Binder, D.K., Croll, S.D., Gall, C.M., Scharfman, H.E., 2001. BDNF and epilepsy: too much of a good thing? Trends Neurosci. 24 (1), 47–53.

Bundman, M.C., Pico, R.M., Gall, C.M., 1994. Ultrastructural plasticity of the dentate gyrus granule cells following recurrent limbic seizures: I. Increase in somatic spines. Hippocampus 4 (5), 601–610.

Chakravarthy, S., Saiepour, M.H., Bence, M., Perry, S., Hartman, R., Couey, J.J., Mansvelder, H.D., Levelt, C.N., 2006. Postsynaptic TrkB signaling has distinct roles in spine maintenance in adult visual cortex and hippocampus. Proc. Natl. Acad. Sci. U. S. A. 103 (4), 1071–1076.

Danzer, S.C., He, X., McNamara, J.O., 2004. Ontogeny of seizure-induced increases in BDNF immunoreactivity and TrkB receptor activation in rat hippocampus. Hippocampus 14 (3), 345–355.

Dashtipour, K., Yan, X.X., Dinh, T.T., Okazaki, M.M., Nadler, J. V., Ribak, C.E., 2002. Quantitative and morphological analysis of dentate granule cells with recurrent basal dendrites from normal and epileptic rats. Hippocampus 12 (2), 235–244.

Dijkhuizen, P.A., Ghosh, A., 2005. BDNF regulates primary dendrite formation in cortical neurons via the PI3-kinase and MAP kinase signaling pathways. J. Neurobiol. 62 (2), 278–288.

Dugich-Djordjevic, M.M., Tocco, G., Lapchak, P.A., Pasinetti, G.M., Najm, I., Baudry, M., Hefti, F., 1992. Regionally specific and rapid increases in brain-derived neurotrophic factor messenger RNA in the adult rat brain following seizures induced by systemic administration of kainic acid. Neuroscience 47 (2), 303–315.

Dugich-Djordjevic, M.M., Ohsawa, F., Okazaki, T., Mori, N., Day, J.R., Beck, K.D., Hefti, F., 1995. Differential regulation of catalytic and non-catalytic trkB messenger RNAs in the rat hippocampus following seizures induced by systemic administration of kainate. Neuroscience 66 (4), 861–877.

Fiala, J.C., Spacek, J., Harris, K.M., 2002. Dendritic spine pathology: cause or consequence of neurological disorders? Brain Res. Brain Res. Rev. 39 (1), 29–54.

Freichel, C., Potschka, H., Ebert, U., Brandt, C., Loscher, W., 2006. Acute changes in the neuronal expression of GABA and glutamate decarboxylase isoforms in the rat piriform cortex following status epilepticus. Neuroscience 141 (4), 2177–2194.

Gorski, J.A., Zeiler, S.R., Tamowski, S., Jones, K.R., 2003. Brain-derived neurotrophic factor is required for the maintenance of cortical dendrites. J. Neurosci. 23 (17), 6856–6865.

Goutan, E., Marti, E., Ferrer, I., 1998. BDNF, and full length and truncated TrkB expression in the hippocampus of the rat following kainic acid excitotoxic damage. Evidence of complex time-dependent and cell-specific responses. Brain Res. Mol. Brain Res. 59 (2), 154–164.

Hanamura, K., Harada, A., Katoh-Semba, R., Murakami, F., Yamamoto, N., 2004. BDNF and NT-3 promote thalamocortical axon growth with distinct substrate and temporal dependency. Eur. J. Neurosci. 19 (6), 1485–1493.

Hariri, A.R., Goldberg, T.E., Mattay, V.S., Kolachana, B.S., Callicott, J.H., Egan, M.F., Weinberger, D.R., 2003. Brain-derived neurotrophic factor val66met polymorphism affects human memory-related hippocampal activity and predicts memory performance. J. Neurosci. 23 (17), 6690–6694.

He, X.P., Minichiello, L., Klein, R., McNamara, J.O., 2002. Immunohistochemical evidence of seizure-induced activation of trkB receptors in the mossy fiber pathway of adult mouse hippocampus. J. Neurosci. 22 (17), 7502–7508.

He, X.P., Kotloski, R., Nef, S., Luikart, B.W., Parada, L.F., McNamara, J.O., 2004. Conditional deletion of TrkB but not BDNF prevents epileptogenesis in the kindling model. Neuron 43 (1), 31–42.

Heldt, S.A., Stanek, L., Chhatwal, J.P., Ressler, K.J., 2007. Hippocampus-specific deletion of BDNF in adult mice impairs spatial memory and extinction of aversive memories. Mol. Psychiatry.

Hering, H., Sheng, M., 2001. Dendritic spines: structure, dynamics and regulation. Nat. Rev. Neurosci. 2 (12), 880–888.

Huang, E.J., Reichardt, L.F., 2003. Trk receptors: roles in neuronal signal transduction. Annu. Rev. Biochem. 72, 609–642.

Kalb, R., 2005. The protean actions of neurotrophins and their receptors on the life and death of neurons. Trends Neurosci. 28 (1), 5–11.

Katoh-Semba, R., Takeuchi, I.K., Inaguma, Y., Ito, H., Kato, K., 1999. Brain-derived neurotrophic factor, nerve growth and neurotrophin-3 selected regions of the rat brain following kainic acid-induced seizure activity. Neurosci. Res. 35 (1), 19–29.

Koyama, R., Yamada, M.K., Fujisawa, S., Katoh-Semba, R., Matsuki, N., Ikegaya, Y., 2004. Brain-derived neurotrophic factor induces hyperexcitable reentrant circuits in the dentate gyrus. J. Neurosci. 24 (33), 7215–7224.

Lahteinen, S., Pitkanen, A., Koponen, E., Saarelainen, T., Castren, E., 2003. Exacerbated status epilepticus and acute cell loss, but no changes in epileptogenesis, in mice with increased brain-derived neurotrophic factor signaling. Neuroscience 122 (4), 1081–1092.

Lan, J., Henshall, D.C., Simon, R.P., Chen, J., 2000. Formation of the base modification 8-hydroxyl-2'-deoxyguanosine and DNA fragmentation following seizures induced by systemic kainic acid in the rat. J. Neurochem. 74 (1), 302–309.

Leite, J.P., Neder, L., Arisi, G.M., Carlotti Jr., C.G., Assirati, J.A., Moreira, J.E., 2005. Plasticity, synaptic strength, and epilepsy: what can we learn from ultrastructural data? Epilepsia 46 (Suppl. 5), 134–141.

Lindholm, D., Carroll, P., Tzimagiogis, G., Thoenen, H., 1996. Autocrine-paracrine regulation of hippocampal neuron survival by IGF-1 and the neurotrophins BDNF, NT-3 and NT-4. Eur. J. Neurosci. 8 (7), 1452–1460.

McAllister, A.K., Lo, D.C., Katz, L.C., 1995. Neurotrophins regulate dendritic growth in developing visual cortex. Neuron 15 (4), 791–803.

McIntyre, D.C., Kelly, M.E., 2000. The parahippocampal cortices and kindling. Ann. N. Y. Acad. Sci. 911, 343–354.

McNamara, J.O., 1999. Emerging insights into the genesis of epilepsy. Nature 399 (6738 Suppl.), A15–A22.

Paxinos, G., Watson, 1997. The Rat Brain in Stereotaxic Coordinates. Academic Press, San Diego.

Pitkanen, A., Sutula, T.P., 2002. Is epilepsy a progressive disorder? Prospects for new therapeutic approaches in temporal-lobe epilepsy. Lancet Neurol. 1 (3), 173–181.

Rensing, N., Ouyang, Y., Yang, X.F., Yamada, K.A., Rothman, S.M., Wong, M., 2005. In vivo imaging of dendritic spines during electrographic seizures. Ann. Neurol. 58 (6), 888–898.

Ribak, C.E., Tran, P.H., Spigelman, I., Okazaki, M.M., Nadler, J.V., 2000. Status epilepticus-induced hilar basal dendrites on rodent granule cells contribute to recurrent excitatory circuitry. J. Comp. Neurol. 428 (2), 240–253.

Rose, C.R., Blum, R., Pichler, B., Lepier, A., Kafitz, K.W., Konnerth, A., 2003. Truncated TrkB-T1 mediates neurotrophin-evoked calcium signalling in glia cells. Nature 426 (6962), 74–78.

Rose, C.R., Blum, R., Kafitz, K.W., Kovalchuk, Y., Konnerth, A., 2004. From modulator to mediator: rapid effects of BDNF on ion channels. Bioessays 26 (11), 1185–1194.

Rossler, O.G., Giehl, K.M., Thiel, G., 2004. Neuroprotection of immortalized hippocampal neurones by brain-derived neurotrophic factor and Raf-1 protein kinase: role of extracellular signal-regulated protein kinase and phosphatidylinositol 3-kinase. J. Neurochem. 88 (5), 1240–1252.

Rudge, J.S., Mather, P.E., Pasnikowski, E.M., Cai, N., Corcoran, T., Acheson, A., Anderson, K., Lindsay, R.M., Wiegand, S.J., 1998. Endogenous BDNF protein is increased in adult rat hippocampus after a kainic acid induced excitotoxic insult but exogenous BDNF is not neuroprotective. Exp. Neurol. 149 (2), 398–410.

Scharfman, H.E., 2005. Brain-derived neurotrophic factor and epilepsy—a missing link? Epilepsy Curr. 5 (3), 83–88.

Scharfman, H.E., Sollas, A.L., Berger, R.E., Goodman, J.H., 2003. Electrophysiological evidence of monosynaptic excitatory transmission between granule cells after seizure-induced mossy fiber sprouting. J. Neurophysiol. 90 (4), 2536–2547.

Schwabe, K., Ebert, U., Loscher, W., 2004. The central piriform cortex: anatomical connections and anticonvulsant effect of GABA elevation in the kindling model. Neuroscience 126 (3), 727–741.

Siddiqui, A.H., Joseph, S.A., 2005. CA3 axonal sprouting in kainate-induced chronic epilepsy. Brain Res. 1066 (1–2), 129–146.

Silhol, M., Bonnichon, V., Rage, F., Tapia-Arancibia, L., 2005. Age-related changes in brain-derived neurotrophic factor and tyrosine kinase receptor isoforms in the hippocampus and hypothalamus in male rats. Neuroscience 132 (3), 613–624.

Sperk, G., 1994. Kainic acid seizures in the rat. Prog. Neurobiol. 42 (1), 1–32.

Tooyama, I., Bellier, J.P., Park, M., Minnasch, P., Uemura, S., Hisano, T., Iwami, M., Aimi, Y., Yasuhara, O., Kimura, H., 2002. Morphologic study of neuronal death, glial activation, and progenitor cell division in the hippocampus of rat models of epilepsy. Epilepsia 43 (Suppl. 9), 39–43.

Van Groen, T., Wyss, J.M., 2003. Connections of the retrosplenial granular b cortex in the rat. J. Comp. Neurol. 463 (3), 249–263.

van Groen, T., Kadish, I., Wyss, J.M., 2004. Retrosplenial cortex lesions of area Rgb (but not of area Rga) impair spatial learning and memory in the rat. Behav. Brain Res. 154 (2), 483–491.

von Bohlen und Halbach, O., Krause, S., Medina, D., Sciarretta, C., Minichiello, L., Unsicker, K., 2006. Regional- and age-dependent reduction in trkB receptor expression in the hippocampus is associated with altered spine morphologies. Biol. Psychiatry 59 (9), 793–800.

Weiss, S., Cataltepe, O., Cole, A.J., 1996. Anatomical studies of DNA fragmentation in rat brain after systemic kainate administration. Neuroscience 74 (2), 541–551.

Whitford, K.L., Dijkhuizen, P., Polleux, F., Ghosh, A., 2002. Molecular control of cortical dendrite development. Annu. Rev. Neurosci. 25, 127–149.

Wirth, M.J., Brun, A., Grabert, J., Patz, S., Wahle, P., 2003. Accelerated dendritic development of rat cortical pyramidal

cells and interneurons after biolistic transfection with BDNF and NT4/5. Development 130 (23), 5827–5838.
Wong, M., 2005. Modulation of dendritic spines in epilepsy: cellular mechanisms and functional implications. Epilepsy Behav. 7 (4), 569–577.
Wyneken, U., Smalla, K.H., Marengo, J.J., Soto, D., de la Cerda, A., Tischmeyer, W., Grimm, R., Boeckers, T.M., Wolf, G., Orrego, F., Gundelfinger, E.D., 2001. Kainate-induced seizures alter protein composition and *N*-methyl-D-aspartate receptor function of rat forebrain postsynaptic densities. Neuroscience 102 (1), 65–74.
Wyneken, U., Marengo, J.J., Villanueva, S., Soto, D., Sandoval, R., Gundelfinger, E.D., Orrego, F., 2003. Epilepsy-induced changes in signaling systems of human and rat post-synaptic densities. Epilepsia 44 (2), 243–246.
Wyss, J.M., Van Groen, T., 1992. Connections between the retrosplenial cortex and the hippocampal formation in the rat: a review. Hippocampus 2 (1), 1–11.
Yan, Q., Radeke, M.J., Matheson, C.R., Talvenheimo, J., Welcher, A. A., Feinstein, S.C., 1997. Immunocytochemical localization of TrkB in the central nervous system of the adult rat. J. Comp. Neurol. 378 (1), 135–157.
Yoo, Y.M., Lee, C.J., Lee, U., Kim, Y.J., 2006. Neuroprotection of adenoviral-vector-mediated GDNF expression against kainic-acid-induced excitotoxicity in the rat hippocampus. Exp. Neurol. 200 (2), 407–417.